Aromaticity in Transition Metal Oxide Structures

R. B. King

Department of Chemistry, University of Georgia, Athens, Georgia 30602

Received June 30, 2000

The concept of aromaticity is useful for understanding the properties of some polyoxometalates containing transition metals such as vanadium, molybdenum, and tungsten having structures based on metal macropolygons and macropolyhedra with M−O−M edges. Thus, the aromatic macrocuboctahedral Keggin ions readily undergo one-electron reductions to highly colored mixed-valence "blues" (e.g., molybdenum blue), whereas the macroicosahedral Silverton ions, $M^{IV}Mo_{12}O_{42}^{8-}$ (M^{IV} = Ce, Th, U), which, like cyclohexane, do not have vertex valence orbitals available for delocalization, do not undergo analogous reduction reactions. A macrohexagon of d^1 vanadium(IV) atoms as V−O−V units has been imbedded into an electronically inactive borate matrix in the ion $[V_6B_{20}O_{50}H_8]^{8-}$. The small β unit for the V−O−V interactions in this V_6 macrohexagon leads to an unprecedented example of high spin aromaticity with a paramagnetism corresponding to four unpaired electrons per V_6 unit in contrast to benzene, which is diamagnetic and hence exhibits low spin aromaticity. The M−O−M interactions in these aromatic metal oxides are closely related to the Cu−O−Cu interactions in the high critical temperature superconducting copper oxides which are essential to the electron transport in these systems.

1. INTRODUCTION

The term "aromatic" was first used by chemists in the early part of the 19th century to designate a specific class of organic substances,[1] which were initially defined and distinguished from those belonging to the aliphatic class by virtue of their pleasant olfactory properties. In this early period the prototypical aromatic compound was already recognized to be benzene, first detected by Michael Faraday in 1825 as a pyrolysis product of whale oil.[2] Subsequent work by Kekulé[3] recognized that the common structural feature of these early aromatic compounds was a hexagonal ring of six carbon atoms.

During the period of nearly two centuries since the original recognition of aromatic compounds, a considerable number of research workers have been engaged in the task of defining and defending various aspects of the concept of aromaticity. However, as recently as 1958 all of the known aromatic compounds were still of a single electronic and topological type containing two-dimensional planar cyclic or polycyclic structural units reducible to systems containing six π-electrons such as benzenoid derivatives, the cyclopentadienide anion, and the tropylium (cycloheptatrienyl) cation.

Since 1958 the range of substances considered to have aromatic character has expanded in several major directions. Thus by 1968 monocyclic hydrocarbons with configurations with from 2 to 30 π-electrons were identified and their aromaticity characterized.[4] Experimental observations on such cyclic hydrocarbons indicated special stability for rings having $4k + 2$ π-electrons and relative instability for rings having $4k$ π-electrons where k is an integer. A more recent development led to an extension of the concept of aromaticity from two-dimensional planar polygonal hydrocarbons to three-dimensional inorganic substances based on deltahedra (polyhedra in which all faces are triangles) in which the maximum numbers of vertices have degrees four or five (the degree of a vertex is the number of edges meeting at that vertex). Examples of such three-dimensional inorganic substances considered to have aromatic properties include deltahedral boranes[5,6] and carboranes[7] of the types $B_nH_n^{2-}$, $CB_{n-1}H_n^-$, and $C_2B_{n-2}H_n$ ($6 \le n \le 12$); octahedral metal carbonyl clusters such as $Rh_6(CO)_{16}$; and bare post-transition element clusters in the Zintl ions obtained in their alloys with alkali metals. Finally within the past few years the concept of two-dimensional aromaticity has been extended from planar networks of fused carbon rings to the surfaces of the large carbon polyhedra of C_{60} and related fullerenes[8] in which all vertices necessarily have degree three.

The discovery of a much more extensive range of compounds regarded as having aromatic properties has led to a broadening of the concept of aromaticity.[9] Originally, aromaticity was associated with a special chemical reactivity. Thus aromatic hydrocarbons such as benzene were considered to be those unsaturated systems which preferentially underwent substitution reactions in preference to addition reactions. Later the idea of special "aromatic" stability came to play a broader role so that aromaticity is now generally equated with the property of lower molecular energy, with a major contribution to the stability of aromatic systems being recognized as arising from delocalization of some of the bonding electrons in these molecules.

Molecular orbital methods have been used to provide a theoretical basis for the concept of aromaticity. Hückel molecular orbital theory[10−13] has been used to express a relationship between a molecular orbital description of structure and aromaticity and leads directly to the criterion of $4k + 2$ π-electrons for the aromatic stability of planar monocyclic complete conjugated hydrocarbons. More re-

10.1021/ci000074u CCC: $20.00
Published on Web 03/02/2001

cently such methods have been extended to polyhedral three-dimensional inorganic structures[14] regarded as aromatic like the two-dimensional aromatic hydrocarbons. Such an extension of Hückel molecular orbital theory requires recognition of its topological foundations so that they can be applied to three-dimensional structures as well as two-dimensional structures. In this connection the author in collaboration with Rouvray[15] first demonstrated in 1977 how graph-theoretical methods arising from the bonding topology of the orbitals participating in the electron delocalization can be used to demonstrate the close analogy between the delocalized bonding in two-dimensional planar aromatic systems such as benzene and that in three-dimensional deltahedral boranes[5,6] and carboranes.[7]

This paper discusses the extension of the concept of aromaticity to certain types of metal oxide frameworks with the ultimate objective of understanding the physical and chemical properties of such structures. The author first applied such ideas to the study of electron delocalization in early transition metal heteropoly- and isopolyoxometalates of molybdenum and tungsten with the objective of understanding their redox properties.[16] The electron delocalization in such structures necessarily involves overlap of metal d orbitals rather than the p orbitals in planar polygonal hydrocarbons such as benzene. These metal−metal interactions are relatively weak since they must occur through oxygen bridges in the M−O−M edges of the metal macropolyhedra in such structures.

More recently this approach has been extended to a study of polyoxovanadates,[17] where structures with a larger number of delocalizable electrons can be obtained because of the greater ease of reduction of the d^0 V(V) to the d^1 V(IV) than of the d^0 Mo(VI) or W(VI) to the d^1 Mo(V) or W(V), leading to polyoxovanadates with a much larger d^1/d^0 metal ratio for vanadium relative to the polyoxometalates of molybdenum and tungsten. In this connection each V^{IV}═O vertex in a polyoxovanadate macropolyhedron is a source of one delocalizable electron, just like a CH vertex in benzene or other planar polygonal hydrocarbons. A polyoxovanadate structure of particular interest is the recently discovered[18,19] polyoxovanadoborate $[V_6B_{20}O_{50}H_8]^{8-}$ in which six V^{IV}═O units are constrained into a planar hexagon by the electronically inactive borate matrix, thus providing a direct comparison between the aromaticity arising from a hexagon of CH units in benzene and that arising from a hexagon of V^{IV}═O units in a polyoxovanadate. In this connection the much weaker V−O−V interactions in $[V_6B_{20}O_{50}H_8]^{8-}$ relative to the C−C interactions in benzene are seen to lead to incomplete electron pairing and paramagnetism in $[V_6B_{20}O_{50}H_8]^{8-}$, in contrast to the complete electron pairing and diamagnetism in benzene. The aromaticity in $[V_6B_{20}O_{50}H_8]^{8-}$ is thus seen to be "high-spin" aromaticity in contrast to the "low-spin" aromaticity in benzene.

Aromaticity in the polyoxometalates is thus seen to depend on relatively weak but significant metal−metal interactions through M−O−M bridges. These metal−metal interactions are closely related to antiferromagnetic M−O−M interactions such as those found in binuclear d^9 Cu(II) compounds.[20,21] Similar M−O−M interactions appear to be involved in the electron transport in the high critical temperature (T_c) copper oxide superconductors.[22]

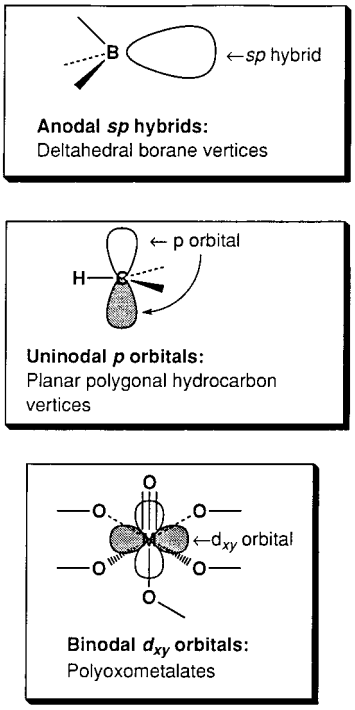

Figure 1. Types of vertex orbitals participating in the delocalization of aromatic systems of various types as classified by their nodalities: (a) the anodal sp hybrid core bonding orbital of a B−H vertex in the deltahedral boranes; (b) the uninodal π-bonding p orbital of a C−H vertex in planar polygonal hydrocarbons such as benzene; (c) the binodal d_{xy} orbital of a metal oxide vertex in polyoxometalates.

2. BINODAL ORBITAL AROMATICITY IN METAL OXIDE STRUCTURES

2.1. Metal Orbital Interactions in Metal Oxide Structures: Relationship to Mixed Valence Systems. Aromaticity may be regarded as stabilization through electron delocalization by interaction between orbitals on adjacent atoms. In this connection the aromaticity in polyoxometalates is three-dimensional involving overlap of binodal transition metal d orbitals (Figure 1).[16] The Hückel treatment of aromatic delocalization may be related to the spectrum of the graph *G*, describing the overall topology of the relevant atomic orbitals by the following equation:[23−26]

$$E_k = \frac{\alpha + x_k\beta}{1 + x_k S} \qquad (1)$$

In eq 1 x_k is an eigenvalue of *G*, E_k is the corresponding molecular orbital energy parameter, and α and β are the standard Hückel parameters. Positive and negative eigenvalues x_k correspond to bonding and antibonding orbitals, respectively.

The binodal aromaticity in polyoxometalates is much weaker than the uninodal aromaticity in planar polygonal hydrocarbons such as benzene or the anodal orbital aromaticity in deltahedral boranes and carboranes (Figure 1).[16] This relates to the fact that in polyoxometalates the vertices furnishing the orbitals participating in the delocalization are relatively far apart, being separated by M−O−M bridges rather than direct M−M bonds corresponding to relatively low β parameters for the polyoxometalates in eq 1. Also note that as β approaches zero, the separation between the energies

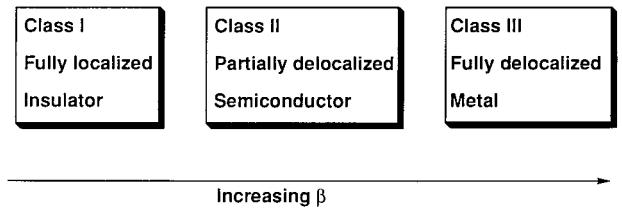

Figure 2. Relationship of β to electrical properties and various types of mixed valence compounds (Robin and Day classification).

of the molecular orbitals can become less than the pairing energies of the electrons filling these molecular orbitals, so that in reduced polyoxometalates all of these molecular orbitals may be filled with single electrons before electron pairing begins. In such a case there is no special stabilization from binodal orbital aromaticity. This situation is exactly analogous to the high spin transition metal complexes obtained from weak field ligands.[27] An intermediate spin situation is found in the "hexagonal" polyoxovanadoborate $[V_6B_{20}O_{50}H_8]^{8-}$. In the case of related polyoxometalate structures the value of β is less for the 3d transition metal vanadium than for the 4d transition metal molybdenum or the 5d transition metal tungsten. For this reason binodal orbital aromaticity is less significant in polyoxovanadates than in polyoxomolybdates and polyoxotungstates, even though more highly reduced polyoxovanadates (i.e., more d^1 V(IV) sites than d^0 V(V) sites) can be obtained than polyoxomolybdates or polyoxotungstates.

Binodal orbital aromaticity only becomes relevant when the d^0 metal sites in unreduced polyoxometalates are reduced to d^1 metal sites in order to obtain electrons for the molecular orbitals generated by overlap of the binodal d orbitals. Such reduced early transition metal polyoxometalates may be related to their interpretation as mixed valence compounds, which Robin and Day[28] classify into the following three classes corresponding to increasing β (Figure 2): class I, fully localized corresponding to an insulator in an infinite system; class II, partially delocalized corresponding to a semiconductor in an infinite system; class III, completely delocalized corresponding to a metal in an infinite system.

ESR studies on the one-electron reduced polyoxometalates $M_6O_{19}^{n-}$ and $XM_{12}O_{40}^{n-}$ suggest class II mixed valence species.[29,30] Although such species are delocalized at accessible temperatures, they behave as localized systems at sufficiently low temperatures similar to semiconductors.

2.2. Polyoxometalate Macropolyhedral Topology: Generation of Degree 4 Polyhedra. The polyoxometalates of interest consist of closed networks of MO_6 octahedra or VO_5 square pyramids where M is a d^0 early transition metal such as vanadium, niobium, molybdenum, or tungsten. These networks may be described by the large polyhedron formed by the metal atoms as vertices. In general, the edges of this macropolyhedron are M−O−M bridges and in most cases there is no direct metal−metal (M−M) bonding. The oxygen atoms are of three types: (1) terminal or external oxygen atoms, which are multiply bonded to the metal (one σ and up to two orthogonal π bonds) and directed away from the macropolyhedral surface; (2) bridging or surface oxygen atoms, which form some or all of the macropolyhedral edges as parts of M−O−M units; (3) internal oxygen atoms, which are directed toward the center of the macropolyhedron.

In metal vertices with two terminal oxygen atoms all of the vertices of the sp^3d^5 manifold of the metal are used for the σ- and π-bonding to the two terminal oxygen atoms and σ-bonding to the bridging and internal oxygen atoms, leaving no orbitals for direct or indirect overlap with other metal vertices of the metal macropolyhedron. Such metal vertices correspond to the saturated CH_2 vertices in cyclohexane and other cycloalkanes. However, in metal vertices with only one terminal oxygen atom, only eight of the nine orbitals of the sp^3d^5 manifold of the metal can be used for σ- and π-bonding to the single terminal oxygen atoms and σ-bonding to the bridging and internal oxygen atoms, leaving one nonbonding d orbital. Thus a metal vertex with only one terminal oxygen atom in a polyoxometalate is analogous to an unsaturated CH vertex with a nonbonding p orbital in a planar aromatic hydrocarbon such as benzene.

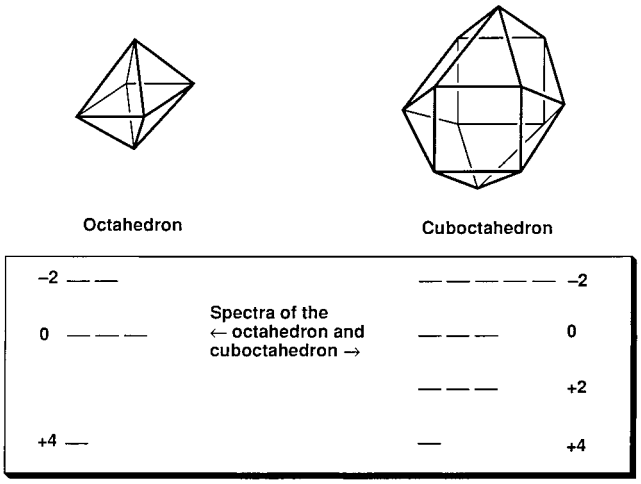

Figure 3. Octahedron and cuboctahedron along with their graph spectra.

The nonbonding *d* orbitals in metal oxide vertices with only one terminal oxygen atom have two orthogonal nodes corresponding to improper 4-fold symmetry. Strict matching of this 4-fold orbital symmetry with the overall macropolyhedral symmetry requires macropolyhedra in which a C_4 axis passes through each vertex. A true three-dimensional polyhedron having C_4 axes passing through each vertex can only have *O* or O_h symmetry, which are the only symmetry point groups with multiple C_4 axes. The only two polyhedra with less than 15 vertices having *O* or O_h symmetry are the regular octahedron and cuboctahedron (Figure 3). These two metal macropolyhedra play key roles in the construction of metal macropolyhedra for early transition metal polyoxometalate structures, particularly polyoxomolybdate and polyoxotungstate structures.

Macropolyhedra which are less symmetrical than the octahedron and cuboctahedron are also found in polyoxometalate structures, particularly polyoxovanadate structures.[17] Of particular interest are macropolyhedra in which all vertices have degree 4 although not necessarily strict C_4 symmetry at each vertex. Broersma, Duijvestijn, and Göbel[31] have shown that three operations (conveniently called the BDG operations) are sufficient to convert the regular octahedron to all possible polyhedra in which all vertices have degree 4 (conveniently called degree 4 polyhedra). The BDG operations are depicted in Figure 4 with descriptive names of their effects on readily recognizable polyhedra such as the octahedron and the square antiprism, the next smallest degree 4 polyhedron. The numbers of topologically distinct degree

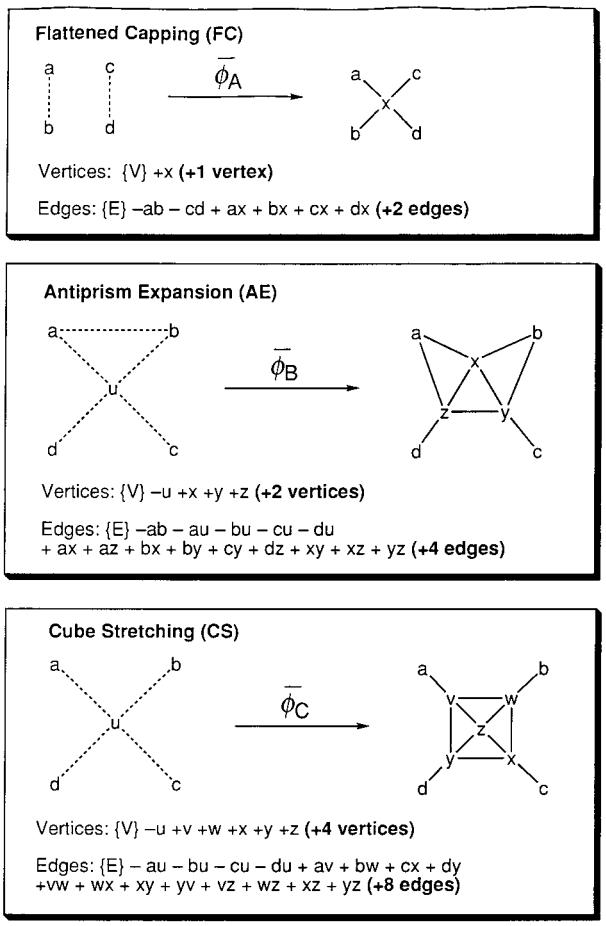

Figure 4. Three operations shown by Broersma, Duijvestijn, and Göbel (BDG)[31] to be sufficient for conversion of a regular octahedron to all possible degree 4 polyhedra.

4 polyhedra have been shown[31] to be 1, 0, 1, 1, 3, 3, 11, 18, 58, and 139 for polyhedra having 6, 7, 8, 9, 10, 11, 12, 13, 14, and 15 vertices, respectively. An important class of degree 4 polyhedra are the antiprisms with two staggered regular polygon faces with n vertices, $2n$ triangular faces, and D_{nd} symmetry. The antiprisms are generated from the octahedron (topologically a trigonal antiprism) by successive applications of the antiprism expansion (AE) operation of Figure 4. Other degree 4 polyhedra of actual or potential chemical significance are the cuboctahedron and the tricapped trigonal prism with the three "vertical" edges deleted. Figure 5 shows the smaller and more recognizable degree 4 polyhedra which can be generated from the regular octahedron by a small number of the BDG operations. Note that the flattened capping operation requires a quadrilateral face and thus cannot be applied to a regular octahedron, so that there are no degree 4 polyhedra with seven vertices.

3. POLYOXOMOLYBDATES AND POLYOXOTUNGSTATES

3.1. Relationship between Structure and Reversible Reducibility of Polyoxomolybdates and Polyoxotungstates. The heteropoly- and isopolyoxometalates of molybdenum and tungsten[32−35] have been known for more than a century and have been studied extensively. Their structures are characterized by networks of MO_6 octahedra in which the molybdenum or tungsten atoms appear in their highest oxidation states in which they have a d^0 configuration. A characteristic of many, but not all, such structures is their reducibility to highly colored mixed oxidation state derivatives often given the trivial names of molybdenum or tungsten "blues". This reducibility of the originally d^0 polyoxometalates can be related to the delocalization of the added electrons(s) in molecular orbitals formed by interaction of nonbonding d orbitals on each of the metal atoms in the MO_6 octahedra forming the polyoxometalate structure and requires that these MO_6 octahedra contain only a single terminal oxygen atom.[36] Nomiya and Miya[37] have used related ideas to develop a structural stability index based on interpenetrating loops of the type −O−M−O−M−O− around the polyoxometalate cage and suggested the analogy of closed loops of this type to macrocyclic π-bonding systems. The ready one-electron reversible reducibility of a colorless to yellow polyoxomolybdate or polyoxotungstate to a highly colored mixed valence "blue" may be viewed as analogous to the one-electron reduction of benzenoid hydrocarbons such as naphthalene or anthracene to the corresponding highly colored radical anion. Pope[36] calls reducible polyoxometalates *type I structures*. An important feature of type I structures is the presence of only $(\mu_n\text{-O})_5\text{MO}$ (M = Mo, W) vertices. Such polyoxometalates can be regarded as a special type of three-dimensional aromatic system, suggesting the applicability of the concept of aromaticity even to special types of metal oxide structures.

The specific building blocks for the reducible polyoxomolybdate and polyoxotungstate structures (type I structures) considered as binodal aromatic systems are based on the following metal macropolyhedra (Figure 3):

A. Macrooctahedron:

$(MO^tO^b_{4/2}O^i_{1/6})_6 = M_6O_{19}^{n-}$ (n = 2, M = Mo):

O^t = one terminal oxygen atom per metal atom;

$O^b_{4/2}$ = one bridging oxygen atom along each of the 12 edges of the macrooctahedron (i.e., (4/2)(6) = 12);

$O^i_{1/6}$ = a single μ_6 oxygen in the center of the M_6 macrooctahedron shared equally among all six metal vertices.

B. Macrocuboctahedron (the so-called "Keggin Structure"):

$(MO^tO^b_{4/2}O^i_{1/3})_{12}X^{n-} = XM_{12}O_{40}^{n-}$ (n = 3−7; M = Mo, W; X = B, Si, Ge, P, Fe^{III}, Co^{II}, Cu^{II}, etc.):

O^t = one terminal oxygen per metal atom;

$O^b_{4/2}$ = one bridging oxygen along each of the 24 edges of the macrocuboctahedron (i.e., (4/2)(12) = 24);

$O^i_{1/3}$ = an OM_3X oxygen bonded to three of the early transition metal atoms. The four oxygen atoms of this type surround the center of the macrocuboctahedron at the vertices of a tetrahedron. The heteroatom X is located in the center of the macrocuboctahedron with tetrahedral coordination to these oxygen atoms.

These type I structures containing only $(\mu_n\text{-O})_5\text{MO}$ vertices can be contrasted with the nonreducible polyoxometalate structures containing only *cis*-$(\mu_n\text{-O})_4\text{MO}_2$ vertices (type II structures in the Pope nomenclature.[36] These structures are necessarily more open since only four of the six oxygens of the MO_6 octahedra can be bridging oxygens. The most stable polyoxometalate structure is the icosahedral Silverton structure $M^{IV}(MoO^t_2O^b_{1/2}O^i_{3/3})_{12}^{8-} = M^{IV}Mo_{12}O_{42}^{8-}$ (M = Ce, Th, U) in which the central metal atom forms an MO_{12} macroicosahedron with the interior oxygen atoms. The central metal atom is a 12-coordinate tetravalent lanthanide

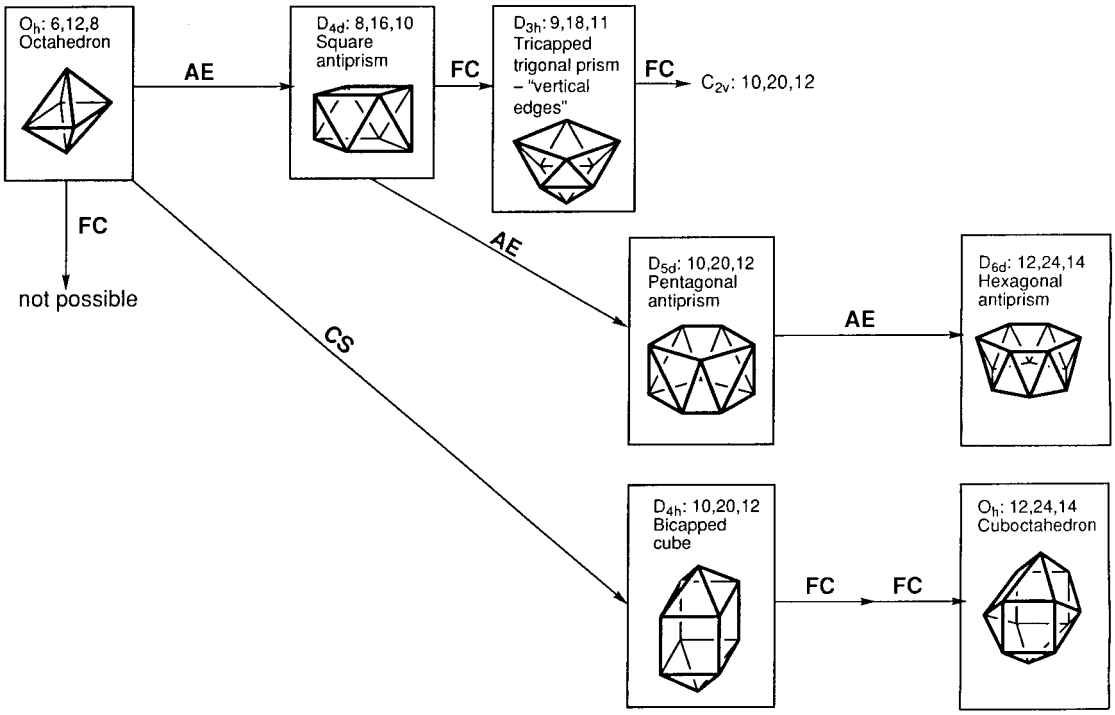

Figure 5. The smaller and more recognizable degree 4 polyhedra which can be generated from the regular octahedron by a small number of the BDG operations depicted in Figure 4.

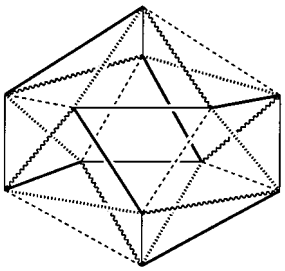

Figure 6. Regular icosahedron with its 30 edges partitioned into five sets of six edges each so that the midpoints of the edges in each set form a regular octahedron. The five sets of six edges each are indicated by different types of lines.

or actinide with accessible f orbitals. The oxygen atoms in the Silverton structure are of the following types:

O^t_2 = two terminal oxygens per metal atom;

$O^b_{1/2}$ = a total of six oxygen atoms ((1/2)(12) = 6) in $MMo_{12}O_{42}^{8-}$, which are located at the vertices of a large octahedron;

$O^i_{3/3}$ = an $OMMo_3$ μ_4-oxygen bonded to three of the molybdenum atoms and to the central metal atom M leading to icosahedral coordination of the latter.

An icosahedron can be decomposed into five equivalent octahedra by partitioning the 30 edges of the icosahedron into five equivalent sets of six edges each so that the midpoints of the edges in each set form a regular octahedron (Figure 6).[38] The vertices of the O^b_6 large octahedron in $MMo_{12}O_{42}^{8-}$ are located above the midpoints of the six edges in one of these octahedral sets of six icosahedron edges.

3.2. Aromaticity in Polyoxomolybates and Polyoxotungstates. The topology of the overlap of the d_{xy} orbitals in type I polyoxometalate structures can be described by a graph *G* whose vertices and edges correspond to the vertices and edges, respectively, of the macropolyhedron (octahedron or cuboctahedron). Equation 1 (section 2) can then be applied to these binodal aromatic systems to relate the spectrum of *G* to the energy parameters of the corresponding bonding and antibonding molecular orbitals. The weakness of the binodal orbital aromaticity in type I polyoxometalates translates into a low β parameter in eq 1.

Figure 3 illustrates the spectra of the octahedron and the cuboctahedron, which are the macropolyhedra in the delocalized polyoxometalates $M_6O_{19}^{n-}$ and $XM_{12}O_{40}^{n}$, respectively. The octahedron is thus seen to have the eigenvalues +4, 0, and −2 with degeneracies 1, 3, and 2, respectively. Similarly the cuboctahedron has the eigenvalues +4, +2, 0, and −2 with degeneracies 1, 3, 3, and 5, respectively. The most positive eigenvalue or *principal eigenvalue* of +4 for both polyhedra arises from the fact that each polyhedron corresponds to a regular graph of valence 4.[39] This highly positive principal eigenvalue corresponds to a highly bonding molecular orbital, which can accommodate the first two electrons upon reduction of the initially d^0 polyoxometalates of the types $M_6O_{19}^{n-}$ and $XM_{12}O_{40}^{n-}$. The reported diamagnetism[40,41] of the two-electron reduction products of the $PW_{12}O_{40}^{3-}$, $SiW_{12}O_{40}^{4-}$, and $[(H_2)W_{12}O_{40}]^{6-}$ anions is in accord with the two electrons being paired in this lowest lying molecular orbital. Thus the overlap of the otherwise nonbonding d_{xy} orbitals in the $M_6O_{19}^{n-}$ and $XM_{12}O_{40}^{n-}$ d^0 early transition metal polyoxometalates creates a low-lying bonding molecular orbital which can accommodate two electrons, thereby facilitating reduction of polyoxometalates of these types.

The spectrum of the cuboctahedron (Figure 3) corresponding to the topology of the $XM_{12}O_{40}^{n-}$ derivatives has not only the single +4 eigenvalue but also the triply degenerate +2 eigenvalue, corresponding to three additional bonding orbitals which can accommodate an additional six electrons. For this reason eight-electron reduction of the $XM_{12}O_{40}^{n-}$ d^0 early transition metal derivatives might be expected to

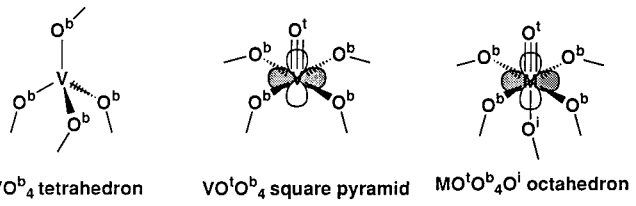

Figure 7. Metal oxide vertexes found in polyoxometalate macropolyhedra (M = V, Mo, W) showing the nonbonding d_{xy} orbitals.

be favorable since eight electrons are required to fill the bonding orbitals of the cuboctahedron, i.e., the four bonding orbitals corresponding to the positive eigenvalues +4 and +2. However, experimental evidence indicates that when six electrons are added to a sufficiently stable $XW_{12}O_{40}$ derivative, rearrangement occurs to a more localized $XW_9^{VI}W_3^{IV}O_{40}^{n-}$ structure in which the three W^{IV} atoms form a bonded triangle[42] with W−W = 2.50 Å, similar to the W−W of 2.51 Å in the tungsten(IV) complex $[W_3O_4F_9]^{5-}$. This bonded W_3 triangle corresponds to one of the triangular faces of the W_{12} macrocuboctahedron in $XW_{12}O_{40}^{n-}$. This rearrangement of the $XW_{12}O_{40}^{n-}$ derivatives to a more localized structure upon six-electron reduction is an indication of the weakness of the binodal orbital aromaticity in these polyoxometalates, corresponding to a low value of β in eq 1. A configuration with three W−W localized two-center two-electron σ-bonds is therefore seen to be more stable than a delocalized configuration with six electrons in the bonding molecular orbitals generated by binodal orbital overlap. Thus if β_σ is defined by the equation

$$\beta_\sigma = (\Delta E_{\text{bonding}} - \Delta E_{\text{antibonding}})/2 \qquad (2)$$

for a W−W σ bond and β_d is the energy unit in eq 5 for overlap of the d_{xy} orbitals on the 12 tungsten atoms (Figure 3), then $\beta_\sigma \gg \beta_d$.

4. POLYOXOVANADATES

4.1. Macropolyhedra Found in Polyoxovanadates: Cages for Small Molecules and Ions. The structural chemistry of polyoxovanadates is richer than that of polyoxomolybdates and polyoxotungstates in the following areas: (1) the variety of metal macropolyhedra and macropolyhedral fragments; (2) the variety of vanadium coordination polyhedra including VO_4 tetrahedra, VO_5 square pyramids, and VO_6 octahedra (Figure 7); (3) the variety of redox states including compounds with only V^V sites, compounds with only V^{IV} sites, and compounds with mixtures of V^V and V^{IV} sites in a variety of ratios. (4) Polyoxovanadate macropolyhedra fragments, particularly those containing VO_5 square pyramids, frequently exhibit "cryptand-clathrate" properties[34] encapsulating various small molecules and ions in species such as $[V_{12}O_{32}(CH_3CN)]^{4-}$, [43] $[H_4V_{18}O_{42}(X)]^{9-}$ (X = Br, I),[44] and $[V_{15}O_{36}(CO_3)]^{7-}$.[44]

The polyoxovanadates contain networks of VO_n (n = 4, 5, 6) polyhedra of the following three types (Figure 7): (1) VO^b_4 tetrahedra with no terminal or internal oxygen atoms (i.e., only surface oxygen atoms); (2) $VO^tO^b_4$ square pyramids with one terminal oxygen atom but no internal oxygen atoms; (3) $VO^tO^b_4O^i$ octahedra with one terminal oxygen atom and one internal oxygen atom.

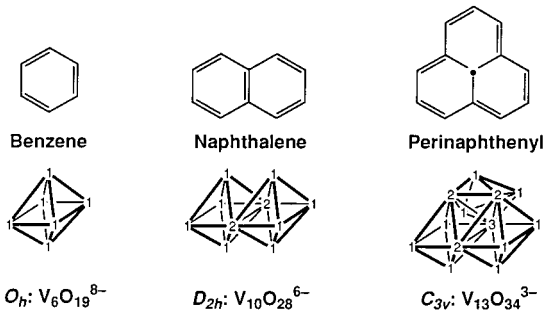

Figure 8. Construction of polyoxovanadates from fusion of vanadium macrooctahedra analogous to the fusion of benzene rings to give naphthalene and perinaphthenyl. Each vertex is labeled according to the number of vanadium macrooctahedra of which it is a part.

The other possible type of MO_6 octahedra, namely, the $MO^t_2O^b_4$ octahedra with two terminal oxygen atoms found in the icosahedral Silverton structures $M^{IV}Mo_{12}O_{42}^{8-}$ (M = Ce, Th, U) = $M^{IV}(MoO^t_2O^b_{1/2}O^i_{3/3})_{12}^{8-}$, is not found in polyoxovanadate structures apparently in accord with the stability of vanadyl derivatives containing $V{\equiv}O^{2+}$ units with only a single multiply bonded oxygen atom.

The VO_n vertices have the following features of interest:

(1) The $VO^tO^b_4$ square pyramids and $VO^tO^b_4O^i$ octahedra have nonbonding d_{xy} orbitals, which can overlap with the d_{xy} orbitals of adjacent $VO^tO^b_4$ square pyramids and $VO^tO^b_4O^i$ octahedra, leading potentially to binodal orbital aromaticity. The d orbitals in VO^b_4 tetrahedra are of too high energy to participate in such overlap so that VO^b_4 vertices can be regarded as "insulating" vertices in a network of "conducting" $VO^tO^b_4$ square pyramids and $VO^tO^b_4O^i$ octahedra.

(2) The vanadium atoms in VO^b_4 vertices are d^0 V^V sites, whereas the vanadium atoms in $VO^tO^b_4$ square pyramids are typically d^1 V^{IV} sites, each of which furnishes one electron for the network of d_{xy} orbitals.

(3) The ability of polyoxovanadates to encapsulate small molecules or ions appears to relate to the "vacant" site trans to the external V≡O bond in the square pyramidal $VO^tO^b_4$ units. Coordination of electron pairs from the encapsulated small molecule or ion to this site effectively converts a square pyramidal $VO^tO^b_4$ site into an octahedral $VO^tO^b_4X$ site (X = donor atom from the encapsulated species).

Polyoxometalates containing a single metal macrooctahedron are known for the heavier congeners of vanadium, namely, niobium and tantalum, with the stoichiometry $M_6O_{19}^{8-}$ (Figure 8: M = Nb, Ta). Fusion of two such vanadium macrooctahedra by sharing one of the macrooctahedral edges gives $V_{10}O_{28}^{6-}$ in which the 28 oxygen atoms are distributed as follows: (a) 8 terminal oxygen atoms, one for each metal vertex belonging only to a single macrooctahedron; (b) 14 edge-bridging oxygen atoms (μ_2-O), one for each of the 14 external edges of the two macrooctahedra; (c) 4 face-bridging oxygen atoms (μ_3-O), one for each of the equivalent pairs of connected edges making triangles between the two octahedra; (d) 2 core oxygen atoms (μ_6-O) in the center of each metal macrooctahedron.

There are two macrotetrahedral cavities between the two vanadium macrooctahedra in $V_{10}O_{28}^{6-}$ of which two of the four faces are faces of the vanadium macrooctahedra. Fusion of a third vanadium macrooctahedron so that one of its eight faces corresponds to a third face of one of these macrotet-

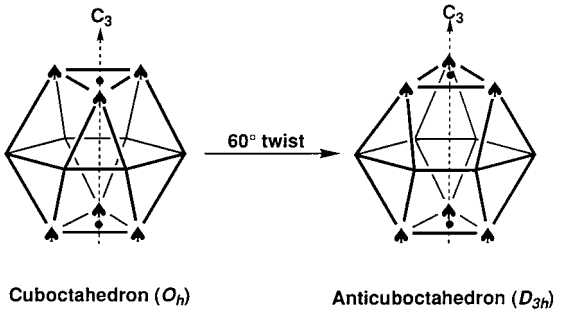

Figure 9. Conversion of the O_h cuboctahedron to the D_{3h} anticuboctahedron by a 60° twist about a C_3 axis. The vertices corresponding to a trigonal antiprism within the cuboctahedron and their conversion to a trigonal prism within the anticuboctahedron by the 60° twist are indicated by spades.

rahedral cavities[45] gives $V_{13}O_{34}^{3-}$ in which the 34 oxygen atoms are distributed as follows: (a) 9 terminal oxygen atoms; (b) 15 edge-bridging oxygen atoms; (c) 7 face-bridging oxygen atoms; (d) 3 core oxygen atoms (μ_6-O) in the center of each of the three metal macrooctahedra.

Fusion of a fourth vanadium macrooctahedron so that one of its faces corresponds to the remaining face of the macrotetrahedral cavity of $V_{13}O_{34}^{3-}$ gives the hypothetical neutral $V_{16}O_{40}$ ($\equiv(V_2O_5)_8$), which has not yet been reported.

The fusion of three-dimensional vanadium macropolyhedra in $V_{10}O_{28}^{6-}$ and $V_{13}O_{34}^{3-}$ may be considered to be analogous to the fusion of two-dimensional benzenoid hexagons in naphthalene and perinaphthenyl (Figure 8). The charge/metal ratio governs the redox behavior rather than the energy parameter of the lowest energy core orbital (i.e., the molecular orbital corresponding to the most positive eigenvalue). Thus the $E°$ values of $V_{10}O_{28}^{6-}$ and $V_{13}O_{34}^{3-}$ with charge/metal ratios of -0.60 and -0.23, respectively, for the first stage of reduction are -0.643 V and $+0.228$ V, respectively,[45] so that $V_{13}O_{34}^{3-}$ is a significantly stronger oxidizing agent than $V_{10}O_{28}^{6-}$.

The second polyhedron with O_h symmetry and less than 15 vertices is the cuboctahedron (Figures 3 and 9). Twisting the "top" triangle of the cuboctahedron depicted in Figure 9 relative to the "bottom" triangle by 60° gives a new polyhedron of D_{3h} symmetry, commonly known as the *anticuboctahedron*. The anticuboctahedron, like the cuboctahedron, has all degree 4 vertices although there are no longer any C_4 axes at any of the vertices in accord with the D_{3h} symmetry of the anticuboctahedron.

The macrocuboctahedron is an important building block for polyoxomolybdates and polyoxotungstates in the so-called "α-Keggin ions" discussed above (section 3). Complete replacement of the Mo^{VI} or W^{VI} atoms in the Keggin ions with V^V atoms would lead to ions with excessive negative charges, e.g., the hypothetical $PV_{12}O_{40}^{15-}$ analogous to $PW_{12}O_{40}^{3-}$. This excessive negative charge can be partially neutralized by capping one or more square faces of the macrocuboctahedron with V^VO^{3+} units (Figure 10). The most stable polyoxovanadate of this type is the bicapped macrocuboctahedral $PV_{14}O_{42}^{9-}$ ($= PV_{12}O_{40}^{15-} + 2VO^{3+}$).

Another polyoxovanadate based on a vanadium macrocuboctahedron is $V_{18}O_{42}^{12-}$ in which all 18 vanadium atoms are in the +4 oxidation state with $VO^tO^b_4$ square pyramidal coordination.[7] The V_{18} macropolyhedron is a macrodeltahedron which can be derived from a V_{12} macrocuboctahedron

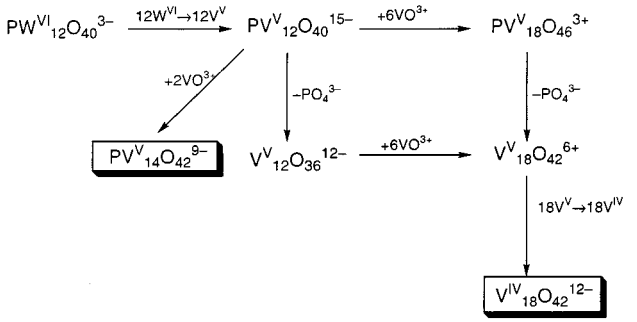

Figure 10. Relationship between the Keggin ion $PW^{VI}_{12}O_{40}^{3-}$ and the polyoxovanadates $PV^V_{14}O_{42}^{9-}$ and $V^{IV}_{18}O_{42}^{12-}$ based on vanadium macrocuboctahedra.

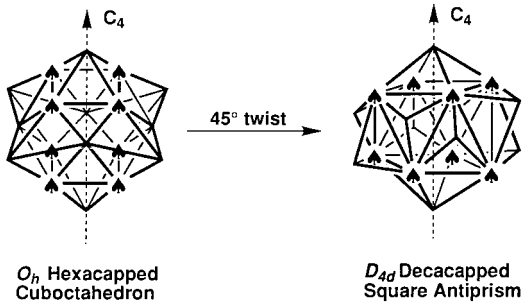

Figure 11. Two 18-vertex deltahedra corresponding to $V_{18}O_{42}^{12-}$ structures, indicating their relationship by a 45° twist about a C_4 axis. The eight vertexes corresponding to the original square antiprism in the D_{4d} polyhedron are indicated by spades.

by capping the six square faces with VO^t units. The relationship of $V_{18}O_{42}^{12-}$ to the Keggin ions such as $PW_{12}O_{40}^{3-}$ is outlined in Figure 10. The "ideal" symmetry of the V_{18} macropolyhedron is O_h, like the cuboctahedron. However, the $V_{18}O_{42}^{12-}$ ion based on a hexacapped cuboctahedron is only formed in solution when tetrahedral anions such as SO_4^{2-} and VO_4^{3-} are present and is stabilized by encapsulating such ions.[44] Encapsulating such tetrahedral ions reduces the symmetry of a hexacapped macrocuboctahedral $V_{18}O_{42}^{12-}$ from O_h to T_d. In the absence of a tetrahedral anion to be encapsulated, the $V_{18}O_{42}^{12-}$ unit adopts D_{4d} symmetry, which is based on a 45° twist of one-half of the hexacapped cuboctahedron to the other half. This polyhedron can be generated from the square antiprism by capping all 10 faces (2 square faces + 8 triangular faces) (Figure 11). Note that both of the 18-vertex polyhedra in Figure 11 are deltahedra. The D_{4d} $V_{18}O_{42}^{12-}$ ion encapsulates spherically symmetrical anions such as Cl^- and Br^-.

Capping three square faces of a V_{12} macrocuboctahedron gives a 15-vertex macropolyhedron exhibiting only C_{2v} or C_{3v} symmetry depending upon the set of three square faces chosen. However, the V_{15} macropolyhedron in $V_{15}O_{36}^{5-}$ has higher D_{3h} symmetry. A deltahedral model of this V_{15} macropolyhedron can be generated from a D_{3h} trigonal prism by the following sequence of processes during which D_{3h} symmetry is preserved at each stage (Figure 12):

(1) The first is capping of the three rectangular faces of the trigonal prism to form the 4,4,4-tricapped trigonal prism, which is the nine-vertex deltahedron found in nine-coordinate complexes and nine-vertex deltahedral borane anions and carboranes;

(2) The next process is removing the three "vertical" edges from the 4,4,4-tricapped trigonal prism to generate a D_{3h}

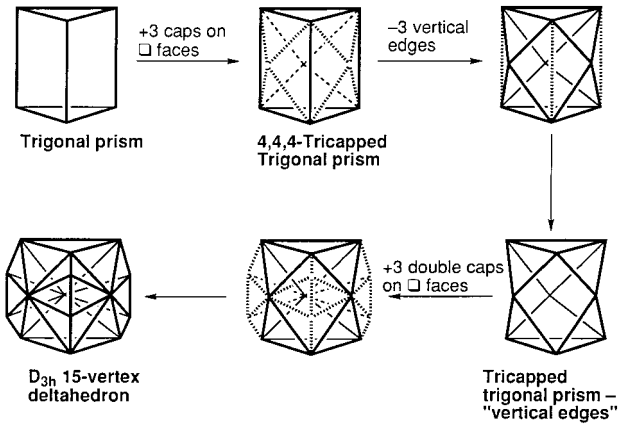

Figure 12. Symmetry-preserving processes for converting the D_{3h} trigonal prism to the likewise D_{3h} 15-vertex deltahedron used to model the $V_{15}O_{36}^{5-}$ structure.

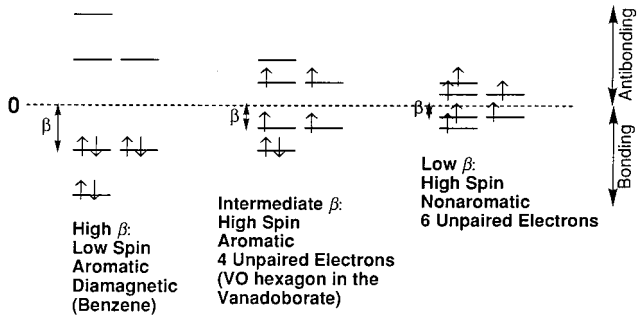

Figure 13. Aromaticity and spin state in a delocalized hexagon as a function of β.

polyhedron with 9 vertices, 18 edges, and 11 faces, which is the only possible nine-vertex polyhedron with all degree 4 vertices. This same nine-vertex polyhedron can be generated from the octahedron by successive antiprism expansion (AE) and flattened capping (FC) (Figure 5).

(3) Capping each of the three quadrilateral faces of the D_{3h} 9,18,11-polyhedron with a *pair* of connected vertices to form a 15-vertex deltahedron is the third process.

The D_{3h} $V_{15}O_{36}^{5-}$ anion is generated in the presence of the D_{3h} carbonate anion, which it encapsulates in $Li_7[V_{15}O_{36}(CO_3)]$.[44]

4.2. Macrohexagonal Polyoxovanadoborates: A High-spin Analogue of Benzene. The vanadium networks in the polyoxovanadates discussed above are all three-dimensional vanadium macropolyhedra, which are not directly analogous to two-dimensional planar organic aromatic molecules. Recently it was discovered that a two-dimensional vanadium(IV) macrohexagon can be imbedded into an electronically inactive borate matrix in the ion $[V_6B_{20}O_{50}H_8]^{8-}$.[18,19] The similarity of the electronically active geometry of this hexagonal polyoxovanadoborate to that of benzene permits a direct comparison of the aromaticity in benzene with that in polyoxometalates. In this connection, density functional calculations at the B3LYP level on the simplified model compound $(O{=}V)_6(\mu\text{-}OH)_{12}$ for $[V_6B_{20}O_{50}H_8]^{8-}$ support a bonding model with the frontier molecular orbitals (MO's) of the vanadium hexagon being a set of six orbitals with predominantly vanadium d character (>70%) well separated in energy from the other MO's.[46] These frontier MO's are highly analogous to a benzene π-system (Figure 13) with an energy gap between the levels, corresponding to β, estimated to be 0.25 eV. Although this value of β is insufficient for complete electron pairing, it is still larger than the energy difference between the lowest and highest of the frontier MO's.

These calculations are consistent with the experimentally determined magnetic properties of the macrohexagonal polyoxovanadoborate. Thus the anion $[V_6B_{20}O_{50}H_8]^{8-}$ has a magnetic moment of 4.1 μ_B,[18] corresponding approximately to four unpaired electrons expected for the high spin aromatic system in Figure 13. This unusual hexagonal polyoxovanadoborate thus provides the first example of aromatic stabilization in a high spin system.

5. COPPER OXIDE SUPERCONDUCTORS

5.1. Structures of Copper Oxide Superconductors: Their Relationship to Polyoxometalates. The superconductors exhibiting the highest known critical transition temperatures (T_c's), namely, the quaternary copper oxides,[47,48] do not have direct Cu−Cu bonding but instead exhibit indirect Cu−O−Cu interactions analogous to the M−O−M interactions in the aromatic polyoxometalates discussed above. These Cu−O−Cu interactions are essential for the electron transport in these materials, which is one of the prerequisites to their superconductivity. From the point of view of aromaticity in metal oxides, the copper oxide superconductors can be considered to be metal-oxide infinite "polymers" with some chemical bonding features analogous to the finite aromatic polyoxometalate structures discussed above. In a crude sense the infinite copper oxide superconductor structures are related to the finite polyoxometalate structures in a manner similar to the relationship of graphite to benzene.

The well-characterized copper oxide superconductors include the following types which can be classified by the geometries of their conducting skeletons in which electron transport takes place:[49,50] (1) the original 40 K superconductors $La_{2-x}M_xCuO_4$ in which the conducting skeleton consists of a single Cu−O plane; (2) the 90 K "123" superconductor $YBa_2Cu_3O_7$ and the 81 K "124" superconductor $YBa_2Cu_4O_8$ in which the conducting skeletons consist of two Cu−O planes braced by single or double Cu−O chains, respectively; (3) the ternary 110 K infinite layer alkaline-earth-deficient superconductors $(Sr_{1-x}Ca_x)_{1-y}CuO_2$; (4) copper oxide superconductors containing a heavy post-transition element in the row Hg → Bi including the homologous series $HgBa_2Ca_{n-1}Cu_nO_{2n+2}$ (n = 1, 2, 3), $Tl_2Ba_2Ca_{n-1}Cu_nO_{2n+4}$ (n = 1, 2, 3), and $Bi_2Sr_2Ca_{n-1}Cu_nO_{2n+4}$ (n = 1, 2, 3), as well as the lead derivatives $Pb_2Sr_2LnCu_3O_8$ (Ln = lanthanide).

The last type of superconductors exhibits the highest T_c values with the maximum reported reliable T_c's being 133, 122, and 115 K for the mercury, thallium, and bismuth derivatives, respectively.

5.2. Chemical Bonding in Copper Oxide Superconductors: Correlation with Electronic Properties. All of the copper oxide superconductors appear to consist of layers of two-dimensional Cu−O conducting skeletons separated by layers of the positive counterions, which can be regarded essentially as insulators. Resistivity[51] and critical magnetic field[52] measurements provide evidence for the two-dimensional nature of the conducting skeletons in these materials. Increasing the rigidity of the two-dimensional conducting skeleton by coupling the Cu−O layers either by

bracing with a Cu−O chain in $YBa_2Cu_3O_{7-y}$ or by close proximity in the higher members of the homologous series $M_2^{III}M_2^{II}Ca_{n-1}Cu_nO_{2n+4}$ (M^{III} = Tl, M^{II} = Ba or M^{III} = Bi, M^{II} = Sr) leads to increases in T_c. The presence of mercury, thallium, or bismuth layers appears to lead to somewhat higher T_c's. This observation coupled with computations of the electronic band structure of $Bi_2Sr_2CaCu_2O_8$[53,54] and the low resistivity of Tl_2O_3 suggests that electron transport may occur in the Bi−O or Tl−O layers as well as the Cu−O layers in the $M_2^{III}M_2^{II}Ca_{n-1}Cu_nO_{2n+4}$ materials. Destruction of the two-dimensional structure of copper oxide derivatives by gaps in the Cu−O planes or by Cu−O chains in the third dimension leads to mixed copper oxides which are metallic but not superconducting[55] such as $La_2SrCu_2O_6$, $La_4BaCu_5O_{13}$, and $La_5SrCu_6O_{15}$.

The following points are of interest concerning the chemical bonding topology of the copper oxide superconductors:[50]

(1) The conducting skeleton is constructed from Cu−O−Cu bonds rather than direct Cu−Cu bonds. The much higher ionic character and thus much lower polarizability and higher rigidity of metal−oxygen bonds relative to metal−metal bonds can be related to the persistence of superconductivity in copper oxides to much higher temperatures than that in metal cluster superconductors which have direct metal−metal bonding.

(2) The required metal−metal interactions are antiferromagnetic interactions between the single unpaired electrons in the d_{xy} orbitals of two d^9 Cu(II) ions separated by an oxygen bridge. Such metal−metal interactions are similar to antiferromagnetic Cu(II)−Cu(II) interactions in discrete binuclear complexes[20,21] and are related to the metal−metal interactions through M−O−M units in the aromatic polyoxometalates discussed above.

(3) The positive counterions in the copper oxide superconductors control the negative charge on the Cu−O skeleton and hence the oxidation states of the copper atoms. Positive counterions, which are "hard" in the Pearson sense[56] in preferring to bind to nonpolarizable bases, such as the lanthanides and alkaline earths, do not contribute to the conductivity. However, layers of the positive counterions mercury, thallium, or bismuth, which are "soft" in the Pearson sense in preferring to bind to polarizable bases, may contribute to the conductivity as noted above.

(4) Partial oxidation of some of the Cu(II) to Cu(III) in the copper oxide superconductors listed above generates holes in the conduction band required for conductivity. This is in accord with Hall effect measurements,[57] which show positive Hall coefficients, indicating that holes rather than electrons are the current carriers. In addition, 28 K superconductors having the general formula $Ln_{2-x}Ce_xCuO_4$ (Ln = Pr, Nd, Sm) are known,[58,59] which have negative Hall coefficients, indicating that mobile electrons are the current carriers. These mobile electrons arise by partial reduction of some of the Cu(II) to Cu(I).

6. SUMMARY

The concept of aromaticity is useful for understanding the properties of some polyoxometalates containing transition metals such as vanadium, molybdenum, and tungsten. The improper 4-fold symmetry (S_4) of the metal d orbitals participating in the delocalization leads to polyhedra of O_h symmetry and all vertices of degree 4 for the basic building blocks of many polyoxometalates exhibiting aromatic properties including the octahedra found in $M_6O_{19}^{n-}$ and the cuboctahedra found in Keggin ions of the type $XM_{12}O_{40}^{n-}$. Less symmetrical polyhedra having only degree 4 vertices can be generated from the simplest such polyhedron, namely, the regular octahedron, by three distinct operations, namely, flattened capping, antiprism expansion, and cube stretching. The concept of aromaticity in the M_{12} polyoxometalates accounts for the experimental observation that the aromatic cuboctahedral Keggin ions readily undergo one-electron reductions to highly colored mixed-valence "blues" (e.g., molybdenum blue), whereas the icosahedral Silverton ions, $M^{IV}Mo_{12}O_{42}^{8-}$ (M^{IV} = Ce, Th, U), which, like cyclohexane, do not have vertex valence orbitals available for delocalization, do not undergo analogous reduction reactions.

Different types of aromatic metal oxide structures are obtained if a network of transition metal atoms, each with a suitable d orbital for delocalization, is imbedded into a matrix of saturated oxide units of elements without such extra orbitals. Using this approach, a macrohexagon of d^1 vanadium(IV) atoms as V−O−V units has been imbedded into a borate matrix in the ion $[V_6B_{20}O_{50}H_8]^{8-}$. The small β unit for the V−O−V interactions in this V_6 hexagon leads to an unprecedented example of high spin aromaticity with a paramagnetism corresponding to four unpaired electrons per V_6 unit, in contrast to benzene, which is diamagnetic and hence exhibits low spin aromaticity.

The M−O−M interactions in these aromatic transition metal oxides may also be interpreted as antiferromagnetic interactions similar to those found in molecular transition metal complexes containing two or more metal atoms interacting through bridging ligands. As such the M−O−M interactions in these aromatic metal oxides are closely related to the Cu−O−Cu interactions in the high critical temperature superconducting copper oxides which are essential to the electron transport in these systems.

ACKNOWLEDGMENT

I acknowledge helpful discussions with Prof. Ian D. Williams, Department of Chemistry, Hong Kong University of Science and Technology, concerning the macrohexagonal polyoxovanadoborate.

REFERENCES AND NOTES

(1) For a description of the early history of aromaticity, see: Snyder, J. P. In *Nonbenzenoid Aromatics*; Snyder, J. P., Ed.; Academic Press: New York, 1969; Chapter 1.
(2) Faraday, M. On New Compounds of Carbon and Hydrogen and on Certain Other Products Obtained During the Decomposition of Oil by Heat. *Philos. Trans. R. Soc. London* **1825**, 440.
(3) Kekulé, A. *Lehrbuch der organischen Chemie*; Enk: Erlangen, 1866; Vol. 2.
(4) Sondheimer, F. The Annulenes. *Acc. Chem. Res.* **1972**, *5*, 81.
(5) Muetterties, E. L.; Knoth, W. H. *Polyhedral Boranes*; Marcel Dekker: New York, 1968.
(6) Muetterties, E. L., Ed.; *Boron Hydride Chemistry*; Academic Press: New York, 1975.
(7) Grimes, R. N. *Carboranes*; Academic Press: New York, 1970.
(8) Kroto, H. W.; Allof, A. W.; Balin, S. P. C_{60}: Buckminsterfullerene. *Chem. Rev.* **1991**, *91*, 1213.
(9) Carey, F. A.; Sundberg, R. J. *Advanced Organic Chemistry. Part A: Structure and Mechanisms*; Plenum: New York, 1977.
(10) Streitwieser, A., Jr. *Molecular Orbital Theory for Organic Chemists*; Wiley: New York, 1961.

(11) Salem, L. *The Molecular Orbital Theory of Conjugated Systems*; Benjamin: New York, 1966.
(12) Dewar, M. J. S. *The Molecular Orbital Theory of Organic Chemistry*; McGraw-Hill: New York, 1969.
(13) Yates, K. *Hückel Molecular Orbital Theory*; Academic Press: New York, 1978.
(14) Aihara, J. Three-Dimensional Aromaticity of Polyhedral Boranes. *J. Am. Chem. Soc.* **1978**, *100*, 3339.
(15) King, R. B.; Rouvray, D. H. Chemical Applications of Group Theory and Topology. VII. A Graph-Theoretical Interpretation of the Bonding Topology in Polyhedral Boranes, Carboranes, and Metal Clusters. *J. Am. Chem. Soc.* **1977**, *99*, 7834.
(16) King, R. B. Chemical Applications of Topology and Group Theory. 25. Electron Delocalization in Early-Transition-Metal Heteropoly- and Isopolyoxometalates. *Inorg. Chem.* **1991**, *30*, 4437.
(17) King, R. B. Chemical Applications of Topology and Group Theory. 27. Topological Aspects of Polyoxovanadate Macropolyhedra. *J. Mol. Struct. (THEOCHEM)* **1995**, *336*, 165.
(18) Williams, I. D.; Wu, M.; Sung, H. H.-Y.; Zhang, X. X.; Yu, J. An Organotemplated Vanadium(IV) Borate Polymer from Boric Acid "Flux" Synthesis, $[H_2en]_4[Hen]_2[V_6B_{22}O_{53}H_8]\cdot 5H_2O$. *Chem. Commun*. **1998**, 2463.
(19) Rose, D. J.; Zubieta, J.; Haushalter, R. Hydrothermal Synthesis and Characterization of an Unusual Polyoxovanadium Borate Cluster: Structure of $Rb_4[(VO)_6\{B_{10}O_{16}(OH)_6\}_2]\cdot 0.5H_2O$. *Polyhedron* **1998**, *17*, 2599.
(20) Doedens, R. J. Structure and Metal−Metal Interactions in Copper(II) Carboxylate Complexes. *Prog. Inorg. Chem.* **1976**, *21*, 209.
(21) Cairns, C. J.; Busch, D. J. Intramolecular Ferromagnetic Interactions in Polynuclear Metal Complexes. *Coord. Chem. Rev.* **1986**, *69*, 1.
(22) King, R. B. The Relationship of the Chemical Bonding Topology of High Critical Temperature Copper Oxide Superconductors to that of the Chevrel Phases and the Ternary Lanthanide Rhodium Borides. *Inorg. Chim. Acta* **1988**, *143*, 15.
(23) Ruedenberg, K. Free-Electron Network Model for Conjugated Systems. V. Energies and Electron Distributions in the FE MO Model and in the LCAO MO Model. *J. Chem. Phys.* **1954**, *22*, 1878.
(24) Schmidtke, H. H. LCAO Description of Symmetric Molecules by Unified Theory of Finite Graphs. *J. Chem. Phys.* **1966**, *45*, 3920.
(25) Schmidtke, H. H. Topological Aspects of Symmetric Molecules. *Coord. Chem. Rev.* **1967**, *2*, 3.
(26) Gutman, I.; Trinajsti'c, N. Graph Theory and Molecular Orbitals. *Top. Curr. Chem.* **1973**, *42*, 49.
(27) Purcell, K. F.; Kotz, J. F. *An Introduction to Inorganic Chemistry*; Saunders: Philadelphia, 1980; Chapter 9.
(28) Robin, M. B.; Day, P. Mixed Valence Chemistry−A Survey and Classification. *Adv. Inorg. Radiochem.* **1967**, *10*, 247.
(29) Launay, J. P.; Fournier, M.; Sanchez, C.; Livage, J.; Pope, M. T. Electron Spin Resonance of Reduced 12-Molybdate Anion and Ground-State Delocalization in Mixed Valence Heteropolyanions. *Inorg. Nucl. Chem. Lett.* **1980**, *16*, 257.
(30) Barrows, J. N.; Pope, M. T. Intermolecular Electron Transfer and Electron Delocalization in Molybdophosphate Heteropoly Anions. *Adv. Chem. Ser.* **1990**, *226*, 403.
(31) Broersma, H. J.; Duijvestijn, A. J. W.; Göbel, F. Generating all 3-Connected 4-Regular Planar Graphs from the Octahedron Graph. *J. Graph Theory* **1993**, *17*, 613.
(32) Pope, M. T. *Hetero and Isopoly Oxometalates*; Springer-Verlag: Berlin, 1983.
(33) Day, V. W.; Klemperer, W. G. Metal Oxide Chemistry in Solution: The Early Transition Metal Polyoxoanions. *Science* **1985**, *228*, 533.
(34) Pope, M. T.; Müller, A. Polyoxometalate Chemistry: An Old Field with New Dimensions in Several Disciplines. *Angew. Chem., Int. Ed.* **1991**, *30*, 34.
(35) *Polyoxometalates: From Platonic Solids to Anti-retroviral Activity*; Pope, M. T., Müller, A., Eds.; Kluwer: Dordrecht, 1994.
(36) Pope, M. T. Heteropoly and Isopoly Anions as Oxo Complexes and Their Reducibility to Mixed-Valence "Blues". *Inorg. Chem.* **1972**, *11*, 1973.
(37) Nomiya, K.; Miwa, M. Structural Stability Index of Heteropoly- and Isopoly-Anions. *Polyhedron* **1984**, *3*, 341.
(38) King, R. B.; Rouvray, D. H. Chemical Applications of Topology and Group Theory. 19. The Even Permutations of the Ligands in Five-Coordinate Complexes Viewed as Proper Rotations of the Regular Icosahedron. *Theor. Chim. Acta* **1986**, *69*, 1.
(39) Biggs, N. L. *Algebraic Graph Theory*; Cambridge University Press: London, 1974; p 14.
(40) Prados, R. A.; Pope, M. T. Low-Temperature Electron Spin Resonance Spectra of Heteropoly Blues Derived from Some 1:12 and 2:18 Molybdates and Tungstates. *Inorg. Chem.* **1976**, *15*, 2547.
(41) Varga, G. M., Jr.; Papaconstatinou, E.; Pope, M. T. Heteropoly Blues. IV. Spectroscopic and Magnetic Properties of Some Reduced Polytungstates. *Inorg. Chem.* **1970**, *9*, 662.
(42) Jeannin, Y.; Launay, J. P.; Sedjadi, M. A. S. Crystal and Molecular Structure of the Six-Electron-Reduced Form of Metatungstate $Rb_4H_8[H_2W_{12}O_{40}]\cdot\sim 18H_2O$: Occurrence of a Metal−Metal Bonded Subcluster in a Heteropolyanion Framework. *Inorg. Chem.* **1980**, *19*, 2933.
(43) Day, V. W.; Klemperer, W. G.; Yaghi, O. M. Synthesis and Characterization of a Soluble Oxide Inclusion Complex, $[CH_3CN\subset(V_{12}O_{32}{}^{4-})]$. *J. Am. Chem. Soc.* **1989**, *111*, 5959.
(44) Müller, A.; Penk, M.; Rohlfing, R.; Krickemeyer, E.; Döring, J. Topologically Interesting Cages of Negative Ions with Extremely High "Coordination Number"; An Unusual Property of V−O Clusters. *Angew. Chem., Int. Ed.* **1990**, *29*, 926.
(45) Hou, D.; Hagen, K. S.; Hill, C. L. Tridecavanadate, $[V_{13}O_{34}]^{3-}$, a New High-Potential Isopolyvanadate. *J. Am. Chem. Soc.* **1992**, *114*, 5864.
(46) Williams, I. D.; Xu, Z.; Lin, Z.; King, R. B., unpublished results.
(47) Poole, C. P.; Datta, T.; Farach, H. A. *Copper Oxide Superconductors*; Wiley: New York, 1988.
(48) Anderson, P. W. *The Theory of Superconductivity in the High T_c Cuprates*; Princeton University Press: Princeton, NJ, 1997.
(49) Williams, J. M.; Beno, M. A.; Carlson, K. D.; Geiser, U.; Ivy Kao, H. C.; Kini, A. M.; Porter, L. C.; Schultz, A. J.; Thorn, R. J.; Wang, H. H.; Whangbo, M.-H.; Evain, M. High Transition Temperature Inorganic Oxide Superconductors: Synthesis, Crystal Structure, Electrical Properties, and Electronic Structure. *Acc. Chem. Res.* **1988**, *21*, 1.
(50) King, R. B. Chemical Structure and Superconductivity. *J. Chem. Inf. Comput. Sci.* **1999**, *39*, 180.
(51) Cheong, S. W.; Fisk, Z.; Kwok, R. S.; Remeika, J. P.; Thomson, J. D.; Gruner, C. Electronic Anisotropy in Single-Crystal La_2CuO_4. *Phys. Rev. B* **1988**, *37*, 5916.
(52) Moodera, J. S.; Meservey, R.; Tkaczyk, J. E.; Hao, C. X.; Gibson, G. A.; Tedrow, P. M. Critical-Magnetic-Field Anisotropy in Single-Crystal $YBa_2Cu_3O_7$. *Phys. Rev. B* **1988**, *37*, 619.
(53) Hybertsen, M. S.; Mattheiss, L. F. Electronic Band Structure of $CaBi_2Sr_2Cu_2O_8$. *Phys. Rev. Lett.* **1988**, *60*, 1661.
(54) Krakauer, H.; Pickett, W. E. Effect of Bismuth on High-T_c Cuprate Superconductors. *Phys. Rev. Lett.* **1988**, *160*, 1665.
(55) Torrance, J. B.; Tokura, Y.; Nazzal, A.; Parkin, S. S. P. Metallic, but not Superconducting, La−Ba (and La−Sr) Copper Oxides. *Phys. Rev. Lett.* **1988**, *60*, 542.
(56) Pearson, R. G. Hard and Soft Acids and Bases. *J. Am. Chem. Soc.* **1963**, *85*, 3533.
(57) Ong, N. P.; Wang, Z. Z.; Clayhold, J.; Tarascon, J. M.; Greene, L. H.; McKinnon, W. R. Hall Effect of $La_{2-x}Sr_xCuO_4$: Implications for the Electronic Structure in the Normal State. *Phys. Rev. B* **1987**, *35*, 8807.
(58) Tokura, Y.; Takagi, H.; Uchida, S. A Superconducting Copper Oxide Compounds with Electrons as the Charge Carriers. *Nature* **1989**, *337*, 345.
(59) Sawa, H.; Suzuki, S.; Watanabe, M.; Akimitsu, J.; Matsubara, H.; Watabe, H.; Uchida, S.; Kokusho, K.; Asano, H.; Izumi, F.; Takayama-Muromachi, E. Unusually Simple Crystal Structure of an Nd−Ce−Sr−Cu−O Superconductor. *Nature* **1989**, *337*, 347.

CI000074U